Stability analysis for the onset of convection in rotating fluid binary mixtures in spherical shells.

<u>Marta Net</u>[*], Ferran Garcia[*] and Juan Sánchez Umbría[*]
Departament de Física Aplicada, Universitat Politècnica de Catalunya, Barcelona, Spain

<u>*Summary*</u>. The stability analysis of the basic conductive state of a rotating binary mixture of two fluids bounded by spherical shells is studied. The Boussinesq approximation of the mass conservation, Navier-Stokes, energy and concentration equations is used, and results for a moderate Ekman number $E = 10^{-3}$ are presented for positive and negative external compositional gradients. Preliminary results are compared with those obtained for a pure fluid in the same range of parameters. They show an important influence of the presence of a mixture on the onset of the convection for solutal Rayleigh numbers R_c at least of the order of the thermal Rayleigh number R_e. On the sphere the leading eigenvectors, which give the patterns of convection, have sectorial structure like those of a pure fluid, although slightly deformed due to the presence of two components.

Introduction

There are a broad range of disciplines in which two-component, or even multicomponent, convection should be taken into account. If the effects of the mixture are ignored a hole group of important phenomena are lost.

The thermal convection in binary fluid spherical shells is a fundamental problem in Astrophysics, Geophysics and Magnetohydrodynamics. For instance, the Earth's magnetic field is generated in its interior by convection driven by thermal and compositional buoyancy, and the thermal convection in the major planets and stars is also affected by the composition of its atmospheres and deep layers.

The onset of convection of a pure fluid subject to radial gravity in rotating spherical shells is well studied (see [1, 2, 3, 4, 5] among many others), but very few is known for a binary mixture. In the first case, the convection breaks the axisymmetry of the conduction state. Then, the first bifurcation is of Hopf type, giving rise to a wave travelling in the azimuthal direction. At moderate E the preferred pattern of convection fills the shell up to high latitudes, keeping the polar regions almost motionless.

The main aim of this work is to study the influence of an externally enforced compositional gradient on the onset of convection of a mixture of two components in a rotating fluid spherical shell. Two possible situations are considered. In the first a stabilizing compositional gradient is imposed. This type of thermosolutal convection predominate, for instance, in large stars having a heated helium-rich core surrounded by lighter hydrogen. In the second the compositional gradient is destabilizing. Such situation occurs in the Earth's core where the solidification of dense metallic iron-nickel crystals on the inner core and the release of light components, such as silicon, drives convection in the outer core more efficiently than thermal gradients [6, 7].

In the first two sections we introduce the formulation of the problem, and the numerical method used to find the leading spectra of the linearized equations, respectively. In the next the neutral stability curves as a function of R_c for Prandtl number $\sigma = 0.1$ and Lewis number $\tau = 0, 0.01$ are shown. In addition the structure of the preferred patterns of convection (eigenvectors) is analyzed. Finally, the paper concludes with a brief outline of the results obtained.

The equations

The extension of the Boussinesq approximation for the mass conservation, Navier-Stokes, temperature, and concentration equations is derived following [8, 9, 10, 11] for a spherical shell of a binary fluid, rotating about an axis at constant angular velocity $\boldsymbol{\Omega} = \Omega \boldsymbol{k}$, and subject to radial gravity $\boldsymbol{g} = -\gamma \boldsymbol{r}$. Differential or internal heating, an external compositional gradient, and the Soret and Dufour effects are included in the formulation of the problem.

The density of the mixture, ρ, is taken constant and equal to its mean value $\overline{\rho}$ in all the terms of the equations but in the gravity term, where it is taken linear with the temperature T and the concentration C, i. e.,

$$\rho(T, C) = \overline{\rho}\left(1 - \alpha(T - \overline{T}) + \beta(C - \overline{C})\right),$$

$\overline{T}$ and $\overline{C}$ being the volume-averaged temperature and concentration of one of the components, respectively.

The physical thermal and the solutal expansion coefficients, defined as

$$\alpha = -\frac{1}{\overline{\rho}}\left(\frac{\partial \rho}{\partial T}\right)_{T=\overline{T}} \quad \text{and} \quad \beta = \frac{1}{\overline{\rho}}\left(\frac{\partial \rho}{\partial C}\right)_{C=\overline{C}},$$

respectively, are considered constant (independent of T and C) like the rest of physical parameters defined below.

We take $\beta > 0$, so the fourth equation is written for the denser component of the mixture. With the above approximation, the complete system in nondimensional form is

$$\boldsymbol{\nabla} \cdot \mathbf{v} = 0, \tag{1}$$

$$(\partial_t + \mathbf{v} \cdot \boldsymbol{\nabla})\mathbf{v} = -\boldsymbol{\nabla}\pi + \nabla^2 \mathbf{v} - 2E^{-1}\boldsymbol{k} \times \mathbf{v} + (T - C)\boldsymbol{r}, \tag{2}$$

$$\sigma\left(\partial_t + \mathbf{v} \cdot \boldsymbol{\nabla}\right)T = (QS^2\tau + 1)\nabla^2 T + QS\tau\nabla^2 C + 3R_i/\sigma, \tag{3}$$

$$\sigma\left(\partial_t + \mathbf{v} \cdot \boldsymbol{\nabla}\right)C = \tau(\nabla^2 C + S\nabla^2 T). \tag{4}$$

Notice that the centrifugal force is neglected because in the Earth's outer core or in the major planets $\Omega^2/\gamma \ll 1$, and that π contains the constant terms coming from $\rho(T, C)$.

To close the problem no-slip boundary conditions for the velocity field ($\mathbf{v} = 0$), perfectly conducting boundaries (constant T), and constant concentration of the components in the outer ($r = r_o$) and inner ($r = r_i$) surfaces are enforced.

To study the onset of convection, the stability analysis of the basic state ($\mathbf{v} = 0, T_c(r), C_c(r)$) is undertaken. In this state the heat transport takes place just by conduction. The equations are written in terms of the perturbation ($\mathbf{u}, \Theta, \Sigma$) of the velocity, temperature and concentration fields, ($\mathbf{v}, T, C$) from the basic state $\mathbf{v} = 0$,

$$T_c(r) = T_0 - \frac{R_i}{2\sigma}r^2 + \left(\frac{R_e - \delta R_i}{\sigma}\right)\frac{\eta}{(1-\eta)^2}\frac{1}{r} \quad \text{and} \quad C_c(r) = C_0 + \frac{R_i S}{2\sigma}r^2 + \left(\frac{\delta R_i S + R_c \tau}{\sigma}\right)\frac{\eta}{(1-\eta)^2}\frac{1}{r}, \quad (5)$$

where $\delta = (1 + \eta)/2(1 - \eta)$ is the mean radius, and $\eta = r_i/r_o$ the radius ratio of the shell ($\eta < 1$).

The nondimensional parameters which appear in the system are the internal Rayleigh (R_i), external Rayleigh (R_e), solutal Rayleigh (R_c), Ekman (E), Prandtl (σ), Lewis (τ), Separation ratio (S), and Dufour (Q) numbers, defined as

$$R_i = \frac{q\gamma\alpha d^6}{3c_p\kappa^2\nu}, \quad R_e = \frac{\gamma\alpha\Delta T d^4}{\kappa\nu}, \quad R_c = \frac{\gamma\beta\Delta C d^4}{\nu D}, \quad E = \frac{\nu}{\Omega d^2},$$

$$\sigma = \frac{\nu}{\kappa}, \quad \tau = \frac{D}{\kappa}, \quad S = \frac{\beta K_T}{\alpha \overline{T}}, \quad Q = \frac{\overline{T}\alpha^2}{c_p\beta^2}\left(\overline{\frac{\partial\mu}{\partial C}}\right)_{p,T},$$

κ being the thermal diffusivity, ν the kinematic viscosity, c_p the specific heat at constant pressure, q the rate of heat due to internal sources per unit mass, K_T the thermal diffusion ratio, D the diffusion coefficient, μ the chemical potential, and $d = r_i - r_o$ the depth of the shell. Notice that $\Delta T = T_i - T_o > 0$ and $\Delta C = C_i - C_o \lessgtr 0$ depending on the sign of the externally enforced compositional gradient. High concentrations of the heavy component in the external layers imply a destabilizing gradient. The equations for a fluid with one component are obtained by putting $C = 0$ and $\tau = 0$.

Moreover, to reduce the number of equations and enforce the continuity condition, the velocity field is substituted by two velocity potentials

$$u = \nabla \times (\Psi \boldsymbol{r}) + \nabla \times \nabla \times (\Phi \boldsymbol{r}), \quad (6)$$

and the equations are rewritten with respect to them.

Numerical methods

The equations for $X = (\Psi, \Phi, \Theta, \Sigma)$ are discretized by expanding the eigenvectors in spherical harmonic series up to degree L, namely

$$X(t, r, \theta, \varphi) = \sum_{l=0}^{L}\sum_{m=-l}^{l} X_l^m(r, t)Y_l^m(\theta, \varphi), \quad (7)$$

with $Y_l^m(\theta, \varphi) = P_l^m(\cos\theta)e^{im\varphi}$, P_l^m being the normalized associated Legendre functions of degree l and order m, and θ denoting the colatitude. In the radial direction, a collocation method on a Gauss-Lobatto mesh is employed.

As in [4], the equations are separated into their azimuthal Fourier coefficients, and the stability of the zero solution of a system of the form

$$\dot{X}_m = \mathcal{A}_m X_m, \quad (8)$$

$\mathcal{A}_m$ being block tridiagonal, is studied. This implies solving the eigenvalue problem $\mathcal{A}_m X_m = \lambda X_m$. Notice that $\mathcal{A}_m$ is real because we separate the equations for the real and imaginary part of the amplitudes. The neutral stability curves correspond to the condition $\mathcal{R}e(\lambda) = 0$. The negative frequencies, which correspond to $\mathcal{I}m(\lambda)$, give positive drifting velocities $c = -\omega_c/m$, i. e., in this case, the waves drift in the prograde direction.

To solve the problem two numerical methods are applied. The first computes the eigenvalues of $\mathcal{A}_m$ by evolving the equation (8) a time interval t. Its solution with initial condition X_m^0 is $\exp(t\mathcal{A}_m)X_m^0$. The eigenvalues, μ, of the linear map $\exp(t\mathcal{A}_m)$ are related to the eigenvalues, λ, of $\mathcal{A}_m$ by $\mu = \exp(t\lambda)$. This transformation maps eigenvalues of maximal real part of $\mathcal{A}_m$ to those of largest modulus of $\exp(t\mathcal{A}_m)$. To find the latter we employ subspace iteration or Arnoldi algorithms (see [12]).

The integration of (8) is performed by a fixed time-step BDF-extrapolation formulae, with initial conditions obtained implicitly with the DLSODPK [13] code, or with a semi-implicit variable-size variable-order (VSVO) method [14]. The scheme of order k is

$$\left(I - \frac{\Delta t}{\gamma_0}\mathcal{A}_m^{(1)}\right)\boldsymbol{x}_m^{n+1} = \sum_{i=0}^{k-1}\frac{\alpha_i}{\gamma_0}\boldsymbol{x}_m^{n-i} + \sum_{i=0}^{k-1}\frac{\Delta t\beta_i}{\gamma_0}\mathcal{A}_m^{(2)}\boldsymbol{x}_m^{n-i},$$

with $\mathcal{A}_m = \mathcal{A}_m^{(1)} + \mathcal{A}_m^{(2)}$, $A_m^{(1)}$ including the diffusion terms, and $A_m^{(2)}$ the rest.

This method follows the envelope that minimizes the thermal Rayleigh number of the neutral stability curves of a given m, but is more demanding from a computational point of view than the second. On the other hand, the time interval
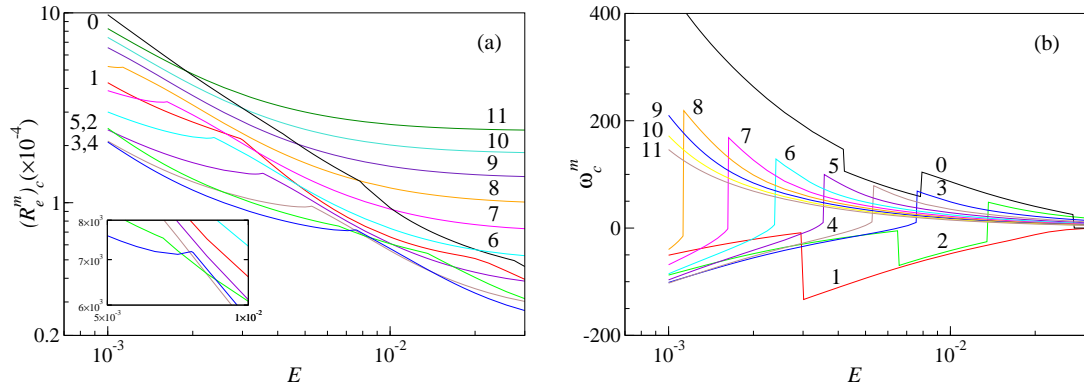
Figure 1: (a) The critical thermal Rayleigh number $(R_e^m)_c$, (b) the critical precession frequency ω_c^m, for each critical mode of azimuthal wavenumber $m = 0, \cdots, 11$, versus E for a pure fluid of $\sigma = 0.1$. The colour criterion is maintained from a) to b).
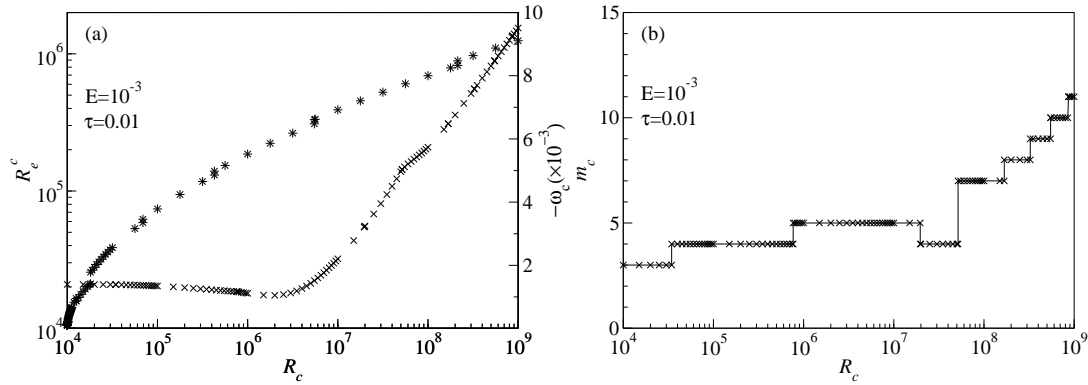
Figure 2: (a) The critical Rayleigh number R_e^c (plotted with $\times$) and the critical precession frequency $-\omega_c$ (plotted with $*$), and (b) the critical wave number m_c plotted versus R_c for $E = 10^{-3}$ and $\tau = 0.01$.

should be selected to be as short as possible to reduce the cost of the evaluation of $\exp(t\mathcal{A}_m)X_m^0$, but large enough to separate the eigenvalues to make their convergence fast.

The second method, based on a double complex shift, was used mainly with $\tau = 0$. It allows to follow the neutral stability curve corresponding to waves of a selected frequency.

Let define $\mathcal{B}_m$ by

$$\mathcal{B}_m = (\mathcal{A}_m - \lambda_s I)^{-1}(\mathcal{A}_m - \bar{\lambda}_s I)^{-1} = \left[(\mathcal{A}_m - \alpha_s I)^2 + \beta_s^2 I\right]^{-1},$$

where the shift $\lambda_s = \alpha_s + i\beta_s$. If λ and $\bar{\lambda}$ are conjugate eigenvalues of $\mathcal{A}_m$, then $[(\lambda - \alpha_s)^2 + \beta_s^2]^{-1}$ and $[(\bar{\lambda} - \alpha_s)^2 + \beta_s^2]^{-1}$ are conjugate eigenvalues of $\mathcal{B}_m$. The shift is changed adaptively to follow the curves.

The eigenvalues of $\mathcal{B}_m$ are found by a subspace iteration or Arnoldi method. This algorithm requires the action of $\mathcal{B}_m$ on a vector $\mathbf{X}$. It is computed by solving the linear system

$$\left[(\mathcal{A}_m - \alpha_s I)^2 + \beta_s^2 I\right](\mathcal{B}_m \mathbf{X}) = \mathbf{X},$$

which is block pentadiagonal. An adapted LU decomposition is employed for this purpose. From the eigenvalues of $\mathcal{B}_m$ and the selected shift (α_s, β_s), the eigenvalues of $\mathcal{A}_m$ are computed. The eigenvectors of both operators are the same.

Notice that the shifting method follows the neutral stability curves very efficiently, but it does not switch over them when mode-crossings are present, so it is very difficult to find the critical parameters automatically without any previous information.

Results

In this paper the calculations are restricted to differential heating with $T_i > T_0$, and positive and negative compositional gradients.

The parameters have been chosen to have physical meaning, although the Ekman numbers used are far from those observed in the nature for computational limitations. They are E down to 10^{-3}, the estimated Prandtl number for the Earth's core [15] $\sigma = 0.1$, $\tau = 0$ and $\tau = 0.01$, and the radius ratio of the Earth's outer core, $\eta = 0.35$. With this assumptions the Dufour effect may be neglected because in liquids it is much smaller than the Soret effect, and we have checked that the later is also negligible if the solutal convection is enforced through external gradients, as in the present case.
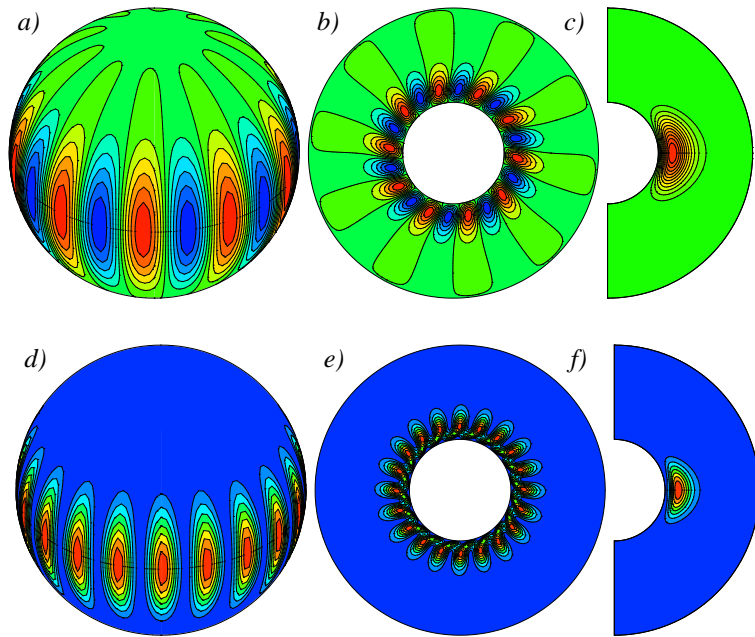
Figure 3: Contour plots of (a-c) the temperature perturbation Θ, (d-f) the kinetic energy density u^2, for $R_c = 5.5 \times 10^8$, $E = 10^{-3}$, $\tau = 0.01$ and $m_c = 10$.

In the first place, the neutral stability curves of the fluid with $\tau = 0$ are computed for Ekman numbers down to $E = 10^{-3}$, to determine the critical thermal Rayleigh number R_e^c, critical precession frequency ω_c and critical wave number m_c, as reference values from which to start the study of the mixture. In fig. 1(a) the critical Rayleigh number of the modes (eigenvectors) of azimuthal wave number $m = 0, \cdots, 11$, $(R_e^m)_c$ is plotted. Their envelope gives R_e^c. At $E = 10^{-3}$, $R_e^c = 2.088 \times 10^4$, $m_c = 3$, and the corresponding frequency, given in Fig. 1(b) by the lower blue line, is $\omega_c = 1.013 \times 10^2$. In this figure the cusps and jumps mean changes of preferred modes of given m.

The preliminary results, obtained with $\tau \neq 0$ and $E = 10^{-3}$, show that the onset of convection gives rises to an azimuthal drifting wave like with $\tau = 0$. Now, the critical thermal Rayleigh number R_e^c depends strongly on the direction of the compositional gradient. However, by comparing this values and also those of ω_c (see Figs. 2 and 4) with those corresponding to $\tau = 0$ (see Fig. 1) it is clear that at least a compositional gradient of the order of the temperature gradient is needed to have important effects due to the solutal convection.

Negative compositional gradients ($C_i > C_o$) are stabilizing, so there is a value of R_c from which R_e^c starts to increase significantly, indicating that the convection is delayed by the presence of a second component. In Fig. 2 this effect may be seen from $R_c \approx 5 \times 10^6$, after a slight fall of R_e^c. In contrast $|\omega_c|$ increases from $R_c = 10^4$ indicating that the wave drifts faster than in a pure fluid.

The well known structure of the modes for $\tau = 0$ changes its shape when R_c and m_c increase (see Fig. 2(b)). The modes, which at $R_c = 10^4$ fill the domain, become much more confined near the inner surface, and their vertical extend is also drastically reduced. Its shape at $R_c = 5.5 \times 10^8$ is plotted in Fig.3. The upper row are the contour plots of Θ on the spherical surface that cuts the vortex near its maximum, the equatorial projection, and the meridional cut taken through the maximum, respectively. The contours plots of the concentration resemble very much this contours. The only difference is an azimuthal phase shift of less than $\pi/2$. The contour plots of the kinetic energy density, u^2, are shown in the second row and display the same characteristics as those of Θ.

Positive and sufficiently large compositional gradients ($C_i < C_o$) are destabilizing, then they may advance the convection with respect to its onset for $\tau = 0$. Notice that with our definition of R_c, this parameter is negative because $\Delta C < 0$.

Fig. 4 contains the neutral stability curves for $E = 10^{-3}$ and $m = 1, \cdots, 8$. In the range of R_c computed there is an interchange of curves for each $m < 8$, whose frequency is shown in fig. 4(b). If the curves cross before the saddle-node ($m = 6, 7$), the jump in the frequency is plotted with a continuous line. Otherwise the two frequencies are not connected. From $R_c = -3.1 \times 10^4$, R_e^c starts to decrease, and the wave number changes from $m = 3$ to $m = 6$. As can be seen in Fig. 4(a), at this point the preferred $m = 6$ mode of convection has already changed and the frequency jumped to $|\omega_c| = 3.82$, so surprisingly the convection becomes almost stationary (see Fig. 4(b)). When $|R_c|$ is increased R_e^c goes on decreasing and even changes sign. Negative R_e^c values indicate that $T_i < T_o$. Then the temperature gradient is stabilizing because the cold fluid occupies the interior layers. Therefore the compositional gradients can trigger the convection even in presence of stabilizing temperature gradients. In this case the azimuthal drift of the waves is very slow. For instance, at $R_c = -2 \times 10^5$ (right limit of the $-R_c$ axis), $|\omega_c| = 0.28$. As $|R_c|$ is increased m_c recovers its starting $m = 3$ value of $R_c = -10^4$.

The contour plots of the critical mode of convection are shown in Fig. 5 for $R_c = -10^5$. They fill the shell as in the pure
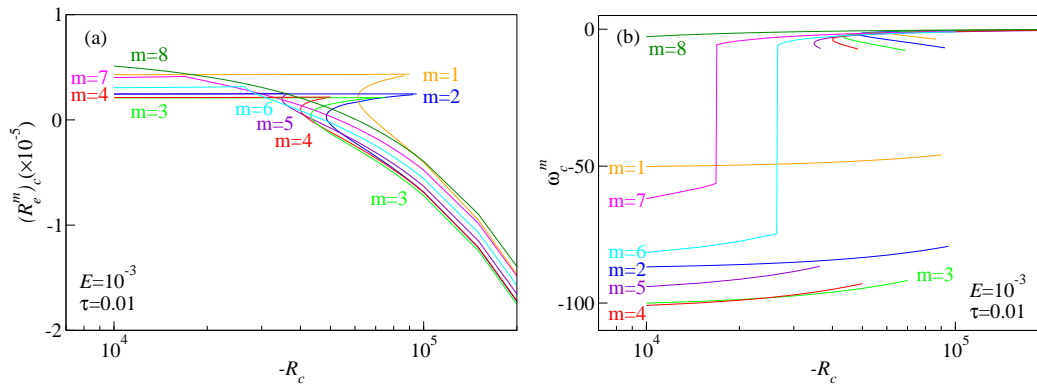
Figure 4: (a) The critical thermal Rayleigh number $(R_e^m)_c$, (b) the critical precession frequency ω_c^m, for each critical mode of azimuthal wavenumber $m = 0, \cdots, 5$, all of them plotted versus the solutal Rayleigh number R_c for $E = 10^{-3}$, $\tau = 0.01$. The colour criterion is maintained from a) to b).
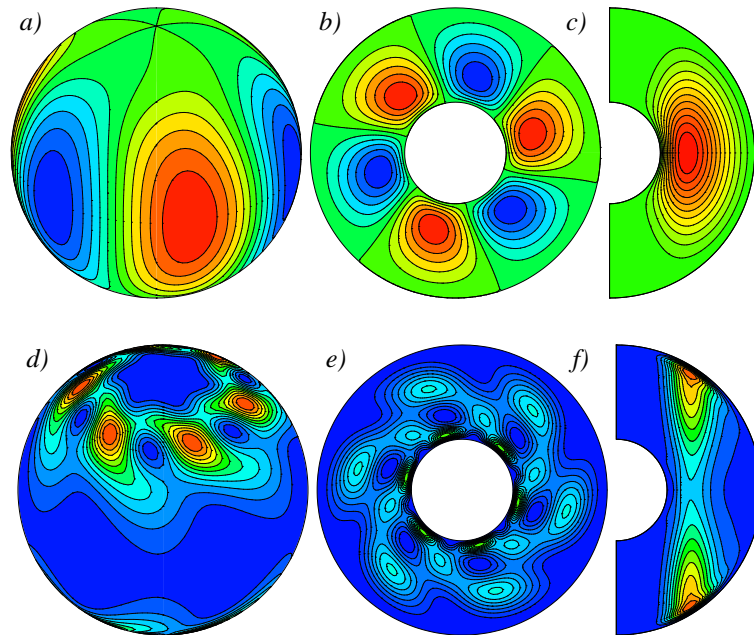
Figure 5: Contour plots of (a-c) the temperature perturbation Θ, (d-f) the kinetic energy density u^2, for $R_c = -10^5$, $E = 10^{-3}$, $\tau = 0.01$, and $m_c = 3$.

fluid, and the kinetic energy density is concentrated at high latitudes near the external boundary. As in the preceding case, the contour plots of the concentration are like those of the temperature perturbation shifted a few degrees.

Conclusions

By comparing the results obtained with a moderate Ekman number $E = 10^{-3}$ with those of a pure fluid we can conclude that:

- In a mixture of fluids of Prantl number $\sigma = 0.1$ and Lewis number $\tau = 0.01$ the solutal effects are important if the enforced compositional gradients are of the order of the temperature gradients, independently of the sign of the former.

- If $C_i > C_o$ (stabilizing gradient) the onset of thermal convection is delayed, i.e. R_e^c is higher than 2.088×10^4 obtained for $\tau = 0$. The precession frequency $|\omega_c|$ and m_c also grow. The pattern of convection consists of vertical vortices confined near the inner boundary. The larger R_c is the shorter they are.

- When $C_i < C_o$ (destabilizing gradient) the compositional gradient reduces the critical value for the onset of convection R_e^c, and it slows down the drift of the waves. The convection can be triggered even in presence of stabilizing temperature gradients. As $|R_c|$ is increased $m_c = 3$ is recovered as for $\tau = 0$.

- In non-rotating or slow-rotating fluids thermosolutal convection gives rises to a great variety of patterns of convection. In fast-rotating fluids it seems that the rotation dominates the dynamics, and the patterns of convection are sectorial like those well known for a pure fluid, even when the convection is driven by the composition.

References

[1] E. Dormy, A. M. Soward, C. A. Jones, D. Jault, P. Cardin, The onset of thermal convection in rotating spherical shells, J. Fluid Mech. 501 (2004) 43–70.

[2] K. Zhang, X. Liao, A new asymptotic method for the analysis of convection in a rapidly rotating sphere, J. Fluid Mech. 518 (2004) 319–346.

[3] K. Zhang, X. Liao, F. Busse, Asymptotic solutions of convection in rapidly rotating non-slip spheres, J. Fluid Mech. 578 (2007) 371–380.

[4] M. Net, F. Garcia, J. Sánchez, On the onset of low-prandtl-number convection in rotating spherical shells: non-slip boundary conditions, J. Fluid Mech. 601 (2008) 317–337.

[5] F. Garcia, J. Sánchez, M. Net, Antisymmetric polar modes of thermal convection in rotating spherical fluid shells at high taylor numbers, Phys. Rev. Lett. 101 (19) (2008) 194501–(1–4).

[6] D. Gubbins, T. G. Masters, J. A. Jacobs, Thermal evolution of the Earth's core, Geophys. J. R. Astron. Soc. 59 (1979) 57–99.

[7] D. E. Loper, P. H. Roberts, Compositional convection and the gravitationally powered dynamo, in: S. A. M. (Ed.), Stellar and Planetary Magnetism, Gordon–Breach, 1983, pp. 297–327.

[8] S. R. de Groot, P. Mazur, Non-equilibrium thermodynamics, Dover Publications, 1962.

[9] L. D. Landau, E. M. Lifshitz, Fluid Mechanics, Pergamon Press, Oxford, 1975.

[10] W. Hort, S. J. Linz, M. Lücke, Onset of convection in binary gas mixtures. role of the dufour effect, Phys. Rev. A 45 (6) (1992) 3737–3747.

[11] R. Simitev, F. H. Busse, Patterns of convection in rotating spherical shells, New Journal of Physics 5 (2003) 97.1–97.20. doi:10.1088/1367-2630/5/1/397.

[12] R. B. Lehoucq, D. C. Sorensen, C. Yang, ARPACK User's Guide: Solution of Large-Scale Eigenvalue Problems with Implicitly Restarted Arnoldi Methods, SIAM, 1998.

[13] A. C. Hindmarsh, ODEPACK, a systematized collection of ODE solvers, in: R. S. S. et al. (Ed.), Scientific Computing, North-Holland, Amsterdam, 1983, pp. 55–364.

[14] F. Garcia, M. Net, B. García-Archilla, J. Sánchez, A comparison of high-order time integrators for the boussinesq navier-stokes equations in rotating spherical shells, J. Comput. Phys. 229 (2010) 7997–8010.

[15] R. A. Secco, H. H. Schloessin, The electrical resistivity of solid and liquid Fe at pressures up to 7 GPa, J. Geophy. Res. B 94 (5) (1989) 5887–5894.